3D THERMAL STEADY-STATE CFD ANALYSIS OF POWER FRICTION LOSSES IN A TURBOCHARGER'S JOURNAL BEARING AND COMPARISON WITH FINITE DIFFERENCE METHOD AND EXPERIMENTATION

M. Deligant[1], P. Podevin[1], F. Vidal[2], W. Tyminski[2], S. Guilain[3], H. Lahjaily[3]
[1]CNAM Paris, France, [2] PSA, Peugeot-Citroen, France, [3] Renault SAS, France

Abstract:

Whether it is due to the CAFÉ commitment or the regulation to come in 2015, but also to the customer requirements, the fuel consumption, and hence the CO2 emissions, become one of the major issue for car manufacturers. One of the most efficient ways to reduce the fuel consumption is to downsize the engines, namely by increasing the engine-specific power and torque, as well as reducing the engine capacity and using turbochargers. In order to keep engine power functioning on a wide area, the turbocharger must have a high performances level. The turbocharger's performances need to be known for the whole range of engine use. Unfortunately, this is not the case for the turbocharger's operation at low speeds (less than 100000 rpm): these speeds are often encountered in automotive applications particularly in urban conditions where fuel consumption optimization is an important issue.

In the CNAM laboratory a series of experiments have been performed on a turbocharger test bench equipped with a torquemeter in the low speed range. Results allow a rough evaluation of friction losses based on the difference between the power delivered to the airflow and the power measured by the torquemeter. It seems that these losses can be accurately obtained through direct calculation.

Solutions for the generalized Reynolds equation with an axial groove device were computed in tables for classical journal bearings used in large machines. These tables compile dimensionless solutions for the Reynolds equation for relative eccentricity between 0.1 and 0.95 and different L/D ratios. Unfortunately, turbocharger journal bearings are weakly loaded and oil viscosity is significant so eccentricity is less than 0.05.

A finite difference method was implemented to solve the isothermal Reynolds equation in order to extend tables for turbocharger applications. This method was validated by recomputing the values in tables and it was applied to the parameters of the turbocharger's journal bearing. As with the classical method, the program authorizes computed solutions for specified L/D ratios and eccentricity. Since the load force is a result of integration of the pressure field, and turbochargers operate with a constant load, relative eccentricity values are to be determined. For that purpose, a simple dichotomy procedure for eccentricity was developed.

This method was then enhanced considering a real inlet layout device with four holes, and applied to the turbocharger's journal bearing for different parameters (inlet oil temperature, inlet oil pressure, rotational speed). The calculated friction power losses seem to be over-estimated by this method due to the high rotational speed and the isothermal hypothesis.

A 3D CFD model using Navier-Stokes mass and energy equations was therefore developed. Calculations were split into two steps. The first step computes pressure and velocity maps with constant temperature. Then the activation of the energy equation and viscous heating allows a temperature map to be computed over all the oil volume. Friction effects result in an increasing oil temperature and decreasing oil viscosity. Thus estimated friction power losses are smaller than with an isothermal method and a comparison with experiments shows more realistic results.

Keywords: turbocharger, friction losses, journal bearings, CFD, THD, hydrodynamic, lubrication

NOMENCLATURE

C	clearance (m) C=Rb-Rj
Ca	friction momentum on the shaft (N.m)
$\overline{C_a}$	dimensionless friction momentum on the shaft
D	bearing diameter (m)
e	eccentricity (m)
f_a	friction number $f_a = \frac{C_a}{RW}$
f	friction coefficient $f = \frac{C_a}{CW}$
h	film thickness (m)
L	bearing length (m)
N	rotational speed of the journal (rpm or Hz)
p	pressure in the film (Pa)
P	power losses (W)
Q	lubricant flow rate (m3 /s)
R	radius (m)
S	Sommerfeld number. $S = \frac{\mu LDN}{W}\left(\frac{R}{C}\right)^2$ with N in Hz
V	linear speed of the journal (m/s)
W	load, external force (N)

Subscripts

b	indicates the bearing
j	indicates the journal

Greek symbols

ε	relative eccentricity $\varepsilon = \frac{e}{C}$
θ	bearing angle (rad)
μ	dynamic viscosity (Pa.s)
ρ	lubricant density (kg/m3)
φ	attitude angle (rad)
ω	angular speed of the journal (rad/s)

CFD : Computational Fluid Dynamic
THD : Thermo-HydroDynamic
HD : HydroDynamic

INTRODUCTION

In order to choose the right turbocharger for a given engine, car manufacturers need to know the turbocharger performances over the whole engine operating range. Currently, turbocharger manufacturers provide a characteristics map issued from tests on a gas stand. Characteristics are not given in the low rotational speed area, because the efficiency of the turbocharger cannot be evaluated with accuracy. The reason is that compressor power is calculated using the first principle of thermodynamics and assuming adiabatic flow which is not valid for this area. Therefore, the turbocharger performances at low speeds must be determined by another way.

Podevin & al [1, 6] worked in the CNAM laboratory with a turbocharger test bench equipped with a torquemeter which gave the power to the shaft, so that they could determine the power given to the air flow by subtracting friction power from mechanical power. These measures could only be taken for either the compressor or the turbine.

Schmitt & al [3] built a test rig, which allowed them to measure friction momentum through a considered system of turbocharger bearings. They put the system into a copy of a turbocharger bearing housing and they were able to directly measure the friction torque. Their experiments give interesting results concerning the friction momentum of journal bearings.

The behavior of journal bearings was described in detail by Osborne Reynolds [2] in 1886. He was the first to publish the formula of hydrodynamic lubrication, henceforth known as the Reynolds equation. His work was based on Mr Tower's experiments, which allowed the prediction of the behavior of journal bearings in a large number of machines.

In this study, the isothermal generalized Reynolds equation was solved for turbocharger conditions through a finite difference method. Then a 3D CFD model using the Navier-Stokes and the energy equation was created using a commercial code.

1. INTRODUCTION

The rotational turbocharger shaft (or rotor) speed is between 10000 rpm and 240000 rpm for automotive engines.

The journal bearing consists of:
- the journal; the surface of the shaft,
- the bearing; the bush part.

The bearing unit is lubricated with standard engine oil 5W30. The oil pressure is between 0.2 MPa and 0.4 MPa, and the temperature between 20°C and 120°C. The bearing unit is composed of two journal bearings parts as showed in blue in Figure 1.

The load is estimated to be equal to the weight of the shaft, the turbine wheel and the impeller: W=1,128 N.

This study focuses on low rotation speeds, less than 110000 rpm, and on the effect of oil temperature. Only one of the two parts is considered as a simple journal bearing with the following characteristics:

Bearing length L = 3.8 mm
Bearing diameter D = 7 mm
Radial clearance C = 15 µm
Load W= 0.564 N

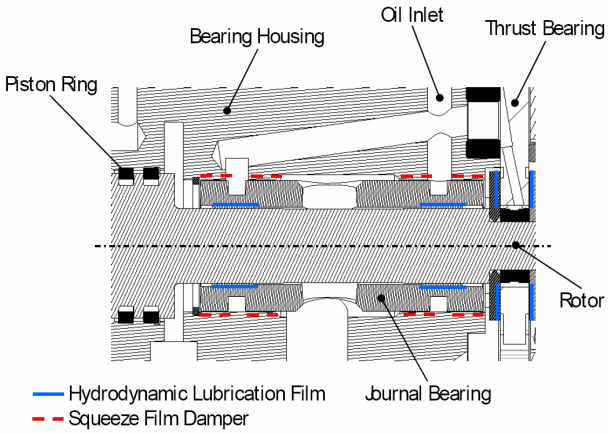

Figure 1 : Sketch of the hydrodynamic bearing unit [3]

The coordinate system and the geometry of the journal bearing are shown on Figure 2. The bearing's radius is Rb and the journal one is Rj. The journal axis Oj is at a distance e from the bearing axis Ob. With geometrical consideration the film thickness h can be defined by the following expressions using bearing coordinates: $\boldsymbol{h = C(1+\varepsilon\cos\theta)}$

The film thickness varies from its maximum value $\boldsymbol{h_0 = C(1+\varepsilon)}$ at the bearing's angle θ = 0 to its minimum value $\boldsymbol{h_0 = C(1-\varepsilon)}$ at θ = π.

Oil dynamic viscosity SAE 5W30 is drawn in Figure 3.

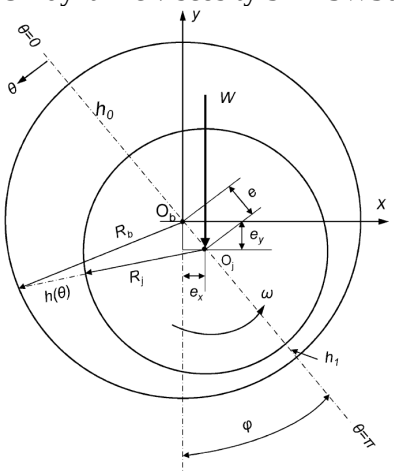

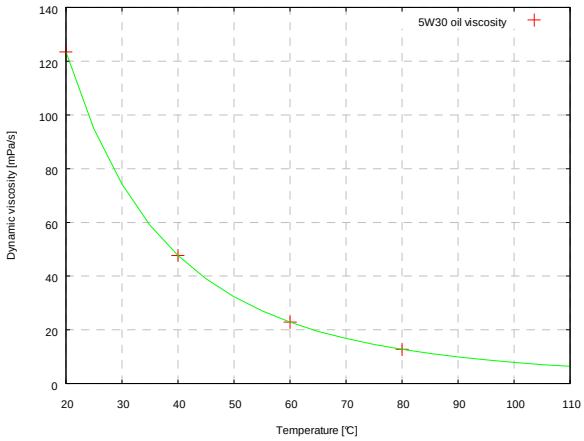

Figure 2 : Schematic geometry and parameters

Figure 3 : Dynamic oil viscosity vs temperature

2. FINITE DIFFERENCE METHOD

2.1. Reynolds equation

Generally, the Reynolds equation - issued from the mass continuity and the momentum conservation equations – is used in lubricant problems dealing with journal bearings, and the following assumptions are made:

- Rigid journal and bearing aligned
- Laminar flow
- Steady state
- Newtonian fluid
- Thickness of oil film very thin compared to other dimensions
- Isothermal flow

The Reynolds [2] equation is:

$$\frac{d}{dx}\left(h^3\frac{dp}{dx}\right)+\frac{d}{dz}\left(h^3\frac{dp}{dz}\right)=6\mu R\omega\frac{dh}{dx}$$

The finite difference method is often used for solving Reynolds equation.

In this paper, the method was applied to the Reynolds equation with turbocharger bearing conditions. Therefore it takes into account the oil supply layout.

Using the following non dimensional variables:

$$\bar{h}=\frac{h}{C}\ ;\theta\ =\ \frac{x}{R}\ ;Z=\frac{z}{L}\ ;P=\frac{p}{6\mu\left(\frac{R}{C}\right)^2}$$

$$\bar{h}=1+\varepsilon\cos\theta$$

The Reynolds equation could be written:

$$\frac{\partial}{\partial\theta}\left(\bar{h}^3\frac{\partial P}{\partial\theta}\right)+\left(\frac{R}{L}\right)^2\frac{\partial}{\partial Z}\left(\bar{h}^3\frac{\partial P}{\partial Z}\right)=\frac{d\bar{h}}{d\theta}$$

In this way it depends on only two parameters, the relative eccentricity and the ratio $\frac{\boldsymbol{R}}{\boldsymbol{L}}$.

So $\bar{\boldsymbol{h}}$ depends only on θ.

$$\frac{\partial^2 P}{\partial \theta^2}+\left(\frac{R}{L}\right)^2\frac{\partial^2 P}{\partial Z^2}+\frac{3}{\bar{h}}\frac{\partial \bar{h}}{\partial \theta}\frac{\partial P}{\partial \theta}=\frac{1}{\bar{h}^3}\frac{d\bar{h}}{d\theta}$$

2.2. Mesh

Reynolds equation is solved on a structured mesh over bearing length and circumference. Circumference is meshed with m intervals and length with n intervals.

$$a=\frac{2\pi}{m-1},\ i\in[1,m]\ \ \theta=ai$$

$$b=\frac{1}{n-1},\ \ j\in[1,n]\ \ Z=bj$$

With a and b small enough, the second order Taylor formula allows the expression of derivative forms through a second order upwind central difference scheme:

$$\frac{\partial P_{i,j}}{\partial \theta}=\frac{P_{i+1,j}-P_{i-1,j}}{2a}$$

$$\frac{\partial^2 P_{i,j}}{\partial \theta^2}=\frac{P_{i+1,j}-2P_{i,j}+P_{i-1,j}}{a^2}$$

$$\frac{\partial^2 P}{\partial Z^2}=\frac{P_{i,j+1}-2P_{i,j}+P_{i,j-1}}{b^2}$$

Then Reynolds equation could be written:

$$\left(\frac{-2}{a^2}+\frac{-2(R/L)^2}{b^2}\right)P_{i,j}+\left(\frac{1}{a^2}-\frac{3}{2a\bar{h}}\frac{d\bar{h}}{d\theta}\right)P_{i-1,j}+$$

$$\frac{(R/L)^2}{b^2}\left[P_{i,j-1}+P_{i,j+1}\right]+\left(\frac{1}{a^2}+\frac{3}{2a\bar{h}}\frac{d\bar{h}}{d\theta}\right)P_{i+1,j}=\frac{1}{\bar{h}^3}\frac{d\bar{h}}{d\theta}$$

$$P_{i,j}=A_iP_{i-1,j}+B_i\left[P_{i,j-1}+P_{i,j+1}\right]+C_iP_{i+1,j}+D_i$$

2.3. Solving

For initial conditions, all relative pressure values were set to 0.

The pressure at the entrance point was set to be constantly at the entrance pressure.

The Reynolds condition for pressure was applied to ensure no negative pressure in the cavitation zone. This condition can be checked on Figure .

The iterative Gauss-Seidel Method was applied to find the solution.

$$P_{i,j}^{r+1}=(1-\Omega)P_{i,j}^{r}+\Omega\left[A_iP_{i-1,j}^{r+1}+B_i\left[P_{i,j-1}^{r+1}+P_{i,j+1}^{r}\right]+C_iP_{i+1,j}^{r}+D_i\right]$$

with Ω the surrelaxation coefficient is between 1.4 and 1.8.0

2.4. Validation

In order to validate the computation, the Reynolds equation was solved for a classical journal bearing with an axial groove. Figure 5, Figure 6 and Figure 7 show the results of computation for a classical journal bearing with the following parameters: D=100mm, L=100mm, N=3000 rpm, μ=0.15Pa·s, ε=0.1

The results are: Sommerfeld number S=1.33, Friction number R/C fa=26.17, Attitude angle Φ=79.4, Load W=25066, Torque=40.2 N·m, so power P=15458 W.

These computations were completed for all values in table [4] with a good accuracy.

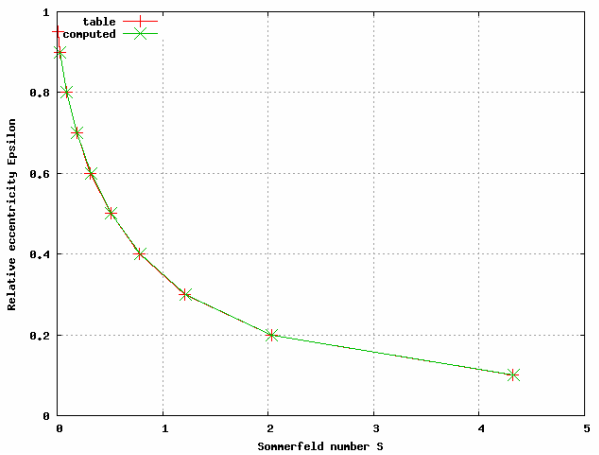

Figure 4 : Relative eccentricity vs. Sommerfeld number for L/D=1/2

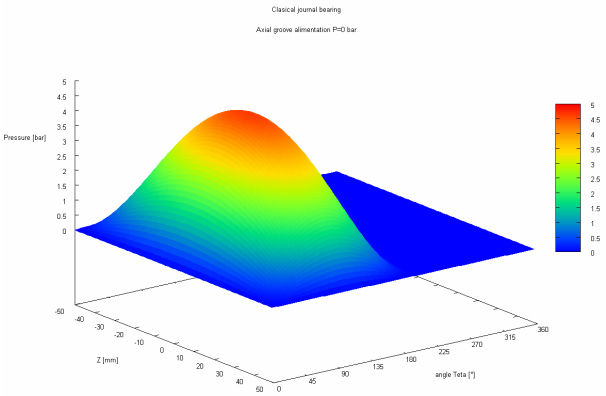

Figure 5 : Shaft pressure map for a classical journal bearing

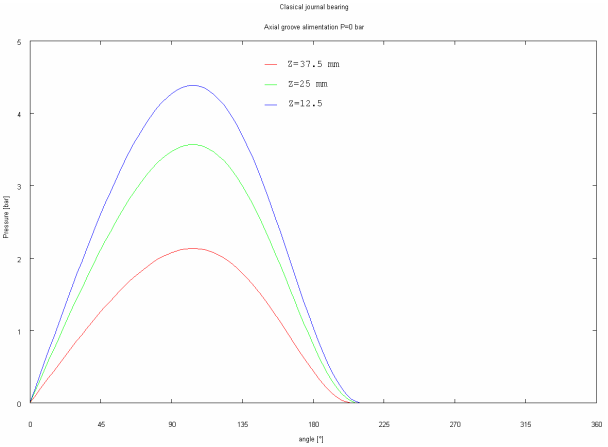

Figure 6 : Shaft pressure vs. angular coordinates

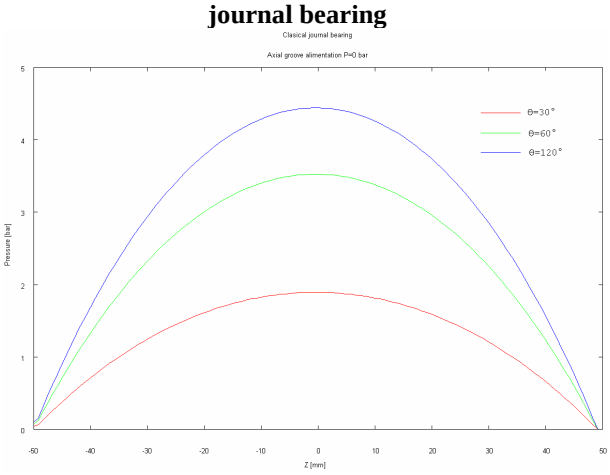

Figure 7 : Shaft Pressure vs. axial position

2.5. Application

Boundary conditions were modified to take into account the four holes' oil supply. Each hole is a zone of constant pressure of 11 radius points. The circumference was divided in 350 points and the length in 60 points, thus a=0.0628 and b=0.0633.

An example of the computed pressure map computed is shown on Figure 8.

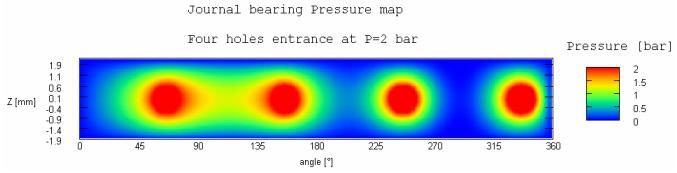

Figure 8 : Shaft pressure map

Zero dimensional solutions for a four hole oil entrance journal bearing with a ratio L/D=0.54 are shown in Figure 9 and Figure 10. For L/D=1/2, tables: results are available for S<4.32. Figure 9 and Figure 10 show results for S up to 65. Figure 10 shows that there is a linear relation between the friction number and Sommerfeld number.

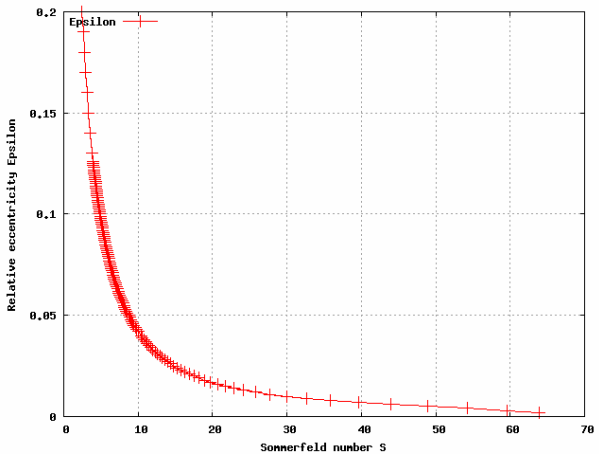

Figure 9 : Relative eccentricity vs. Sommerfeld number

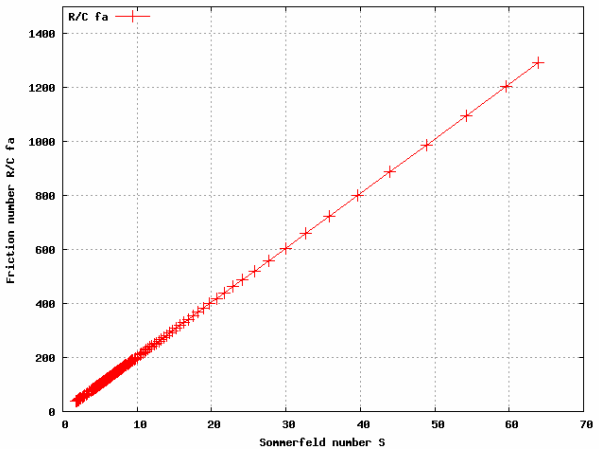

Figure 10 : Friction number vs. Sommerfeld number

2.6. Results

The model was applied to compute turbocharger journal bearing characteristics for several temperatures and speeds. Figure 11 and Figure 12 present results of torque and power vs. rotational speed for four temperatures. Characteristics were extracted for the given value of load W = 0.564 N by dichotomy. Results are similar to those of reference [5], values could be compared using the oil viscosity ratio.

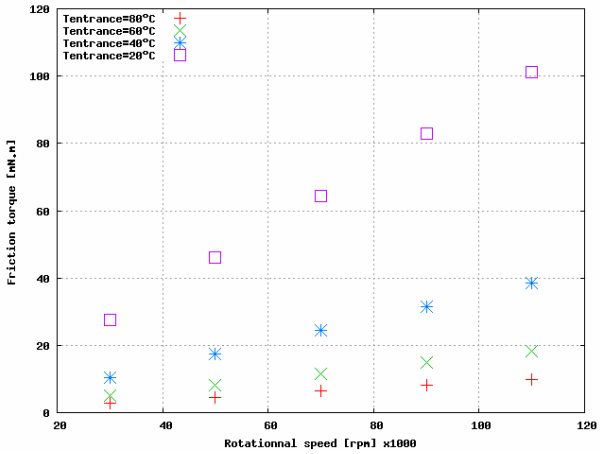

Figure 11 : Friction torque vs. Rotational speed

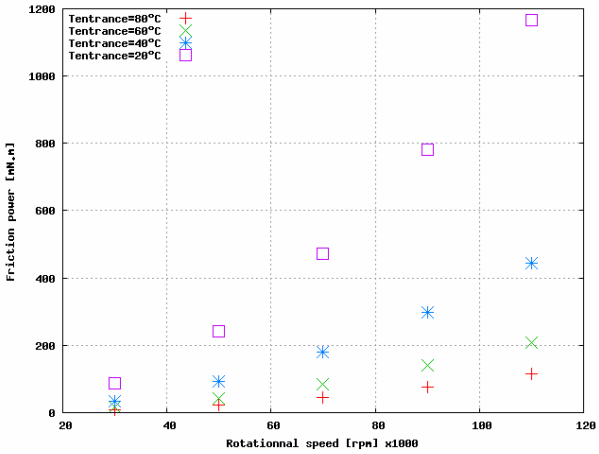

Figure 12 : Friction power vs. rotational speed

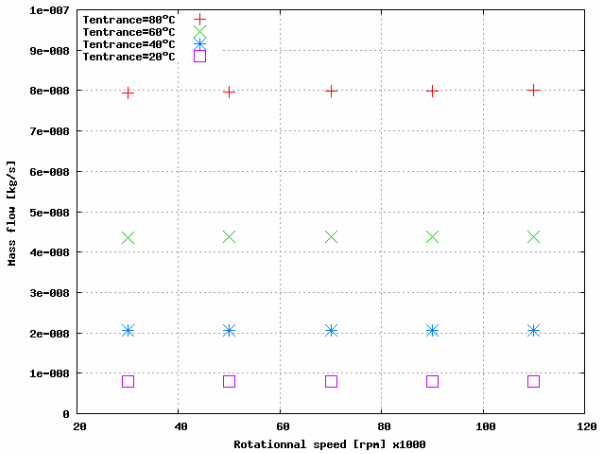

Figure 13 : Mass flow vs. rotational speed

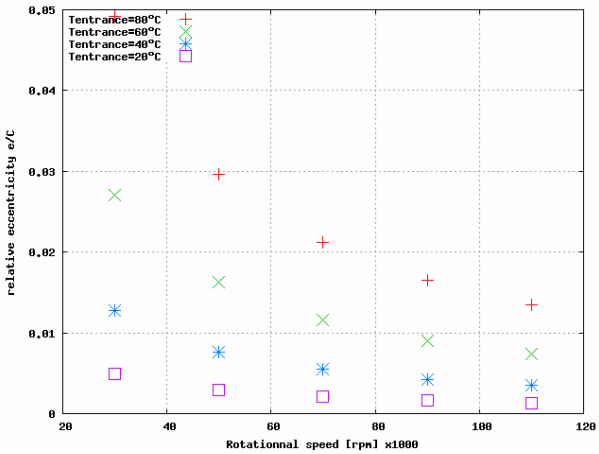

Figure 14 : Relative eccentricity vs. rotational speed

Computations show that the friction torque could be approximated by a linear relation with the rotational speed and the power by a second order relation with rotational speed.

Figure 13 show that results of mass flow rate vs. rotational speed are very low.

According to reference [4], in the case of a short bearing, the zero dimension mass flow $\frac{\boldsymbol{Q}}{\boldsymbol{LCV}} = \boldsymbol{\varepsilon}$, this could explain the low mass flow rates because the bearing is weakly loaded so relative eccentricity is low, less than 0.05. For instance for T=80°C, N=30000 rpm, ε = 0.049, zero dimension mass flow is 0.126618 so the flow is 7.94 10-8 kg/s.

However, the friction power calculated by this method seems too high to be representative of the reality. Seeing that only one bearing has been considered, the total bearings friction losses should be 1 kW when shaft is rotating at 110 000 rpm.

Reference [1] measured the total friction power losses, including thrust bearing. This power is 150 W at 30000 rpm and up to 450 W at 110000 rpm for entrance temperature 40°C. Though this method is very useful and very quick in a lot of cases, it couldn't be used in for turbochargers due the high dependence of viscosity with temperature.

In order to enhance this method, the effective viscosity is often calculated. For that it is assumed that 85 % of heat is evacuated by oil flow, friction power is compared to heat transfer by oil and effective oil viscosity is found iteratively. In this case it seems impossible to apply this method due to the very low mass flow computed. This remark leads us to think that heat transfer does not only occur due to the flow through the bearing, but also due to conduction inside the bush and external flow in damper film.

3.CFD

This paragraph presents a CFD analysis using the commercial code ANSYS Fluent.

3.1. Model & assumption

The shaft is supposed to be running aligned so half a bearing with a symmetry condition was considered. The flow is supposed to be laminar. Isothermal calculation is undertaken to initialize before thermal calculation. This allows the validity of the model to be checked comparing isothermal results with those of finite difference method.

Oil dynamic viscosity and density are functions of temperature. Piecewise linear functions with 40 points were chosen for the computations.

The clearance between the bush and the bearing unit allows oil flow around the bush which dampens vibrations and cools down the bearing.

This, combined with finite difference results concerning mass flow, leads to the hypothesis that most of the cooling is supplied by conduction through the bush instead of convection through the flow.

The program solves the Navier-Stokes equations. Mesh was generated for several given eccentricities by a commercial meshing program GAMBIT.

3.2. Boundaries conditions

Reynolds condition is applied on the pressure map. For each iteration, a function set the relative pressure to 0 Pa for all cells with negative pressure.

The outlet pressure condition is set to be 0. Lubricant is supplied by four 1.4 mm diameter holes under a pressure of 0.2MPa.

There are 4 thermal boundary conditions: Entrance temperature, Backflow temperature, Adiabatic journal, Isothermal bearing. The bearing temperature is set to be equal to the oil entrance temperature due to the cooling flow in the clearance.

3.3. Mesh

The volume was meshed with 15 intervals through the thickness. Other lengths were meshed with a size of 0.075 mm. So the total number of cells is 111 600. The maximum cell squish is 0.696.

Meshing parameters were chosen after a parametric study on the number of cells through thickness and the length.

Isothermal friction torque, thermal friction torque and shaft temperature were studied to determine the minimum number of cells through thickness required to obtain a well-converged result. The difference between the value for mesh interval 15 and mesh interval 30 is around 0.2% for isothermal friction momentum and shaft temperature: it is less than 1.5% for thermal friction momentum, so 15 intervals were chosen to give good results with a reasonable computation time (figures 15, 16 and 17).

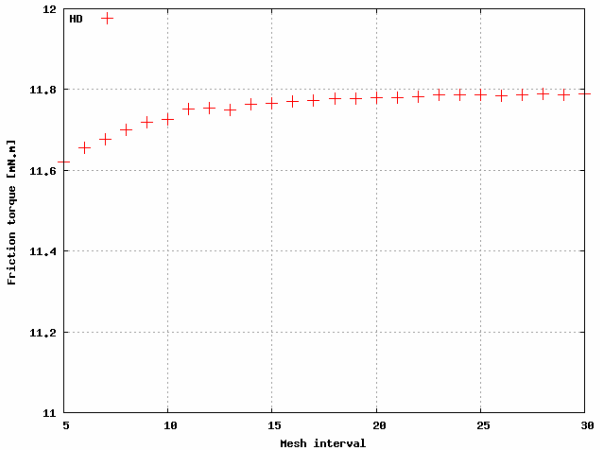

Figure 15 : Isothermal friction torque vs. number of cells through thickness

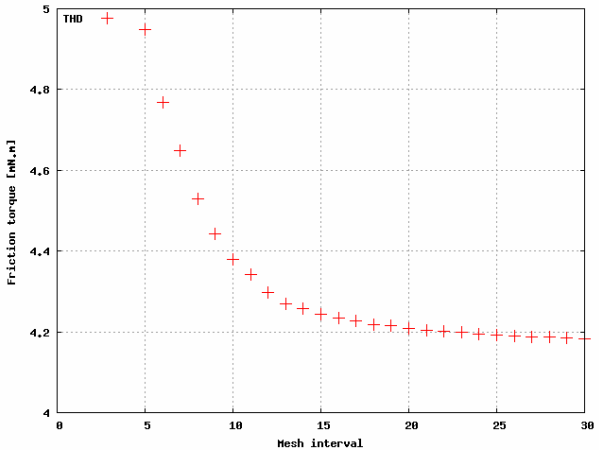

Figure 16 : Thermal friction torque vs. number of cells through thickness

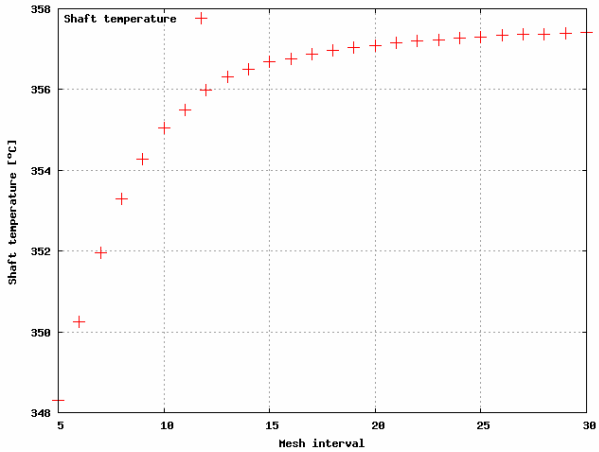

Figure 17 : Thermal shaft temperature vs. number of cells through thickness

3.4. Convergence

Criterions for convergence were set as following: Velocity residuals: 1e-5, Energy residuals: 1e-8, Difference between mass flow inlet and mass flow outlet <= 1%

Momentum and shaft temperature convergence are also monitored to ensure that the saved values are really the final converged value.

3.5. Results

In this paragraph all the results for a journal bearing of length of 3.8 mm are presented. The friction torque and friction power vs. rotational speed were drawn for parametric values of oil

entrance temperature and with isothermal CFD and thermal CFD. Figure 18 shows an example of the computed pressure map.

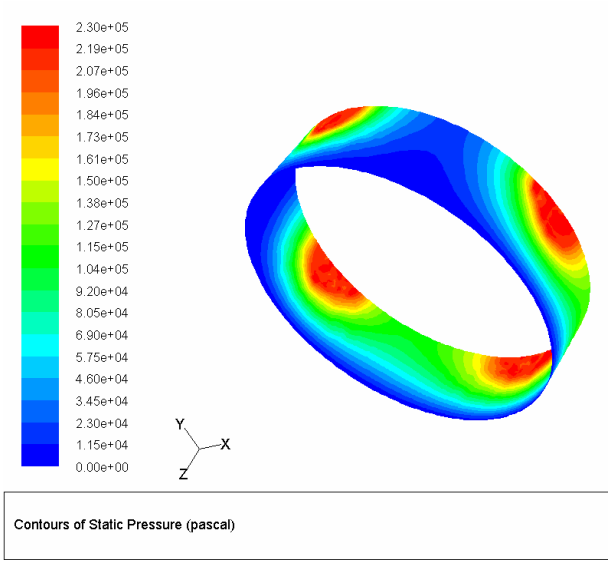

Figure 18 : Pressure map on the shaft

Isothermal results were very close those obtained with the finite difference method, although these calculations were longer, it confirms the validity and efficiency of the finite difference method, in the case of isothermal hypothesis.

Figure and Figure show the difference between the result of isothermal and thermal hydrodynamic calculation THD for an oil lubricating temperature entrance of 40°C. For a rotational speed of 110000 rpm, friction torque is nearly divided by 5.

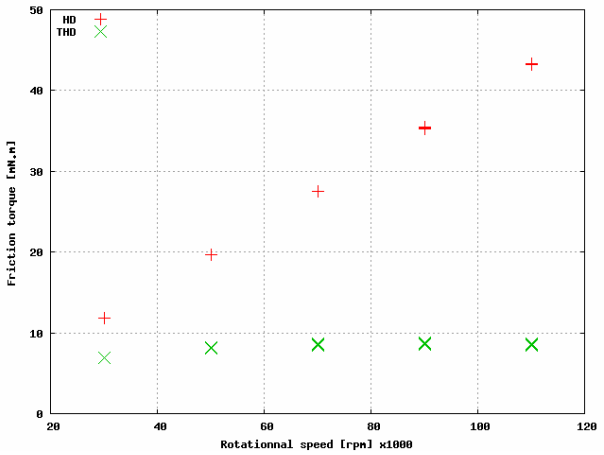

Figure 19 : Comparison of friction torque between isothermal and thermal CFD for entrance temperature=40°C

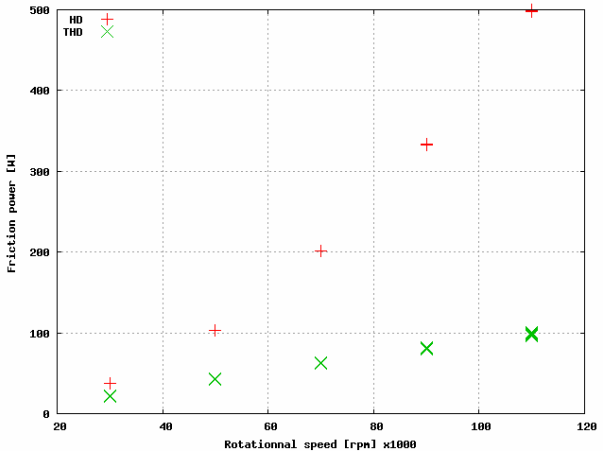

Figure 20 : Comparison of friction power between isothermal and thermal CFD for entrance temperature=40°C

Figure 21 and Figure 22 present all the results of the isothermal calculations. These figures are similar to Figure 11 and Figure 12. A linear relation could be found for each momentum vs. rotational speed, and a second order relation could be found for power vs. rotational speed. These results validate the isothermal CFD model compared with the finite difference method.

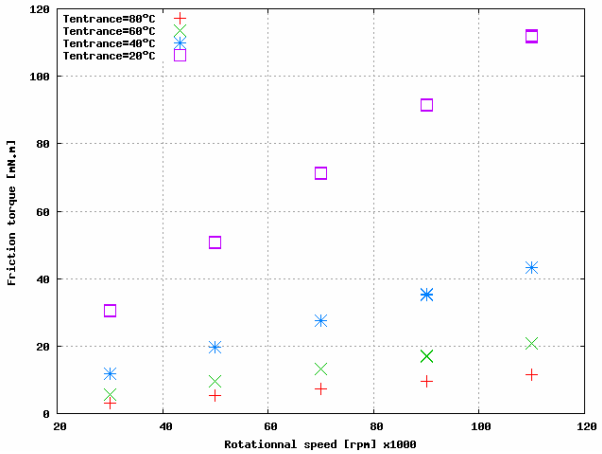

Figure 21 : Isothermal friction torque vs. Rotational speed

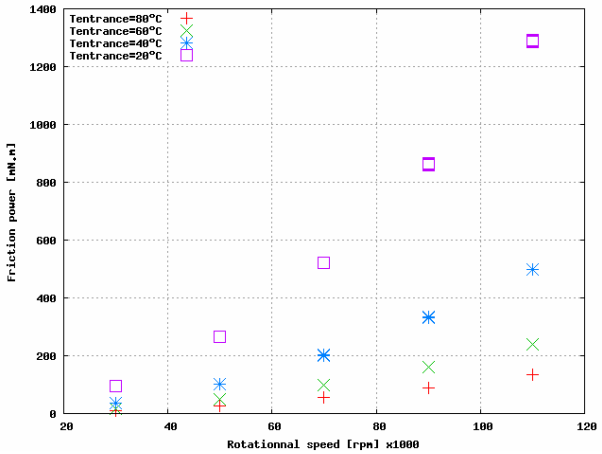

Figure 22 : Isothermal friction power vs. Rotational speed

Considering thermal hydrodynamic calculations, Figure 23, the friction torque seems to be decreasing with rotational speed for entrance temperatures 20 and 40 °C.

Figure 25 and Figure 26 show with more detail the influence of shaft temperature and corresponding viscosity on friction torque and friction power. This can be explained by viscous heating which makes oil temperature increase and oil viscosity diminishes: this tends to reduce the friction momentum.

Momentum results seem to be in agreement with the measurements of reference [3].

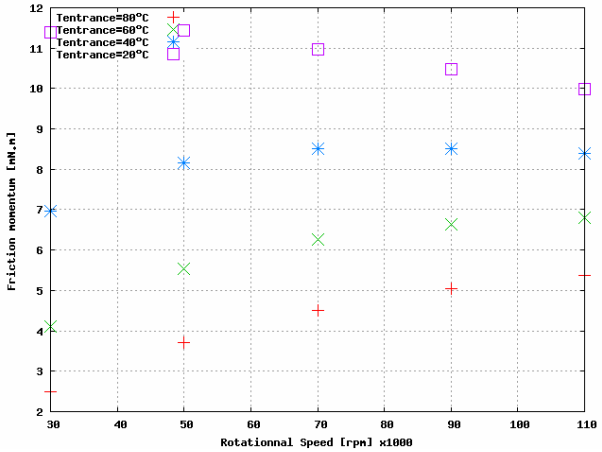

Figure 23 : Thermal friction torque vs. Rotational speed

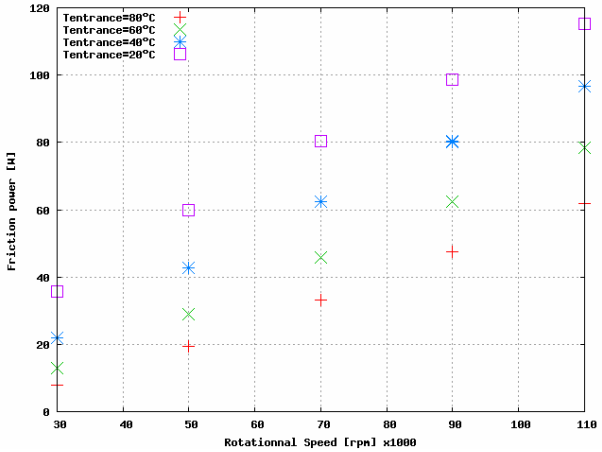

Figure 24 : Thermal friction power vs. Rotational speed

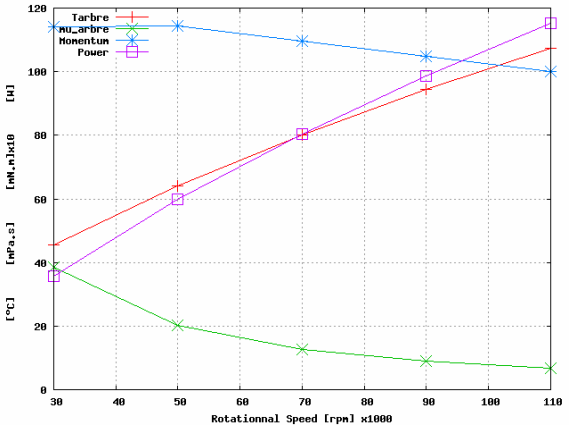

Figure 25 : Friction power, friction torque, shaft temperature and corresponding viscosity vs. rotational speed for entrance temperature = 20°C

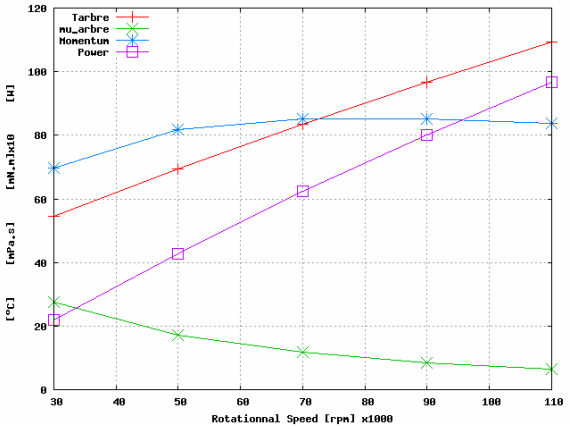

Figure 26 : Friction power, friction torque, shaft temperature and corresponding viscosity vs. rotational speed for entrance temperature = 40°C

Figure 27 and Figure 28 summarize the results of power and torque vs. shaft temperature. On Figure 28, for a given entrance temperature, friction power seems to be linear with shaft temperature.

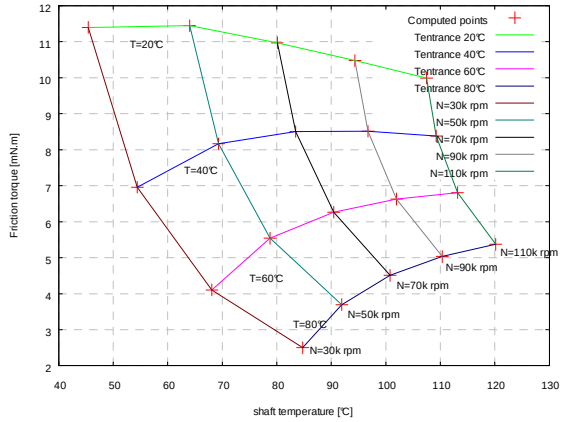

Figure 27 : Thermal friction torque vs. oil temperature on shaft with constant entrance temperature and rotational speed

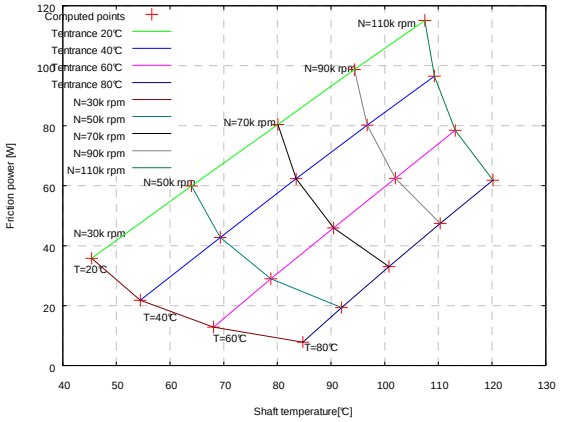

Figure 28: Thermal friction power vs. oil temperature on shaft with constant entrance temperature and rotational speed

Figure 29 to Figure 30 summarize the results of power and torque vs. shaft equivalent viscosity on shaft. These figures insist on the viscosity effects. One could remark that the variation of viscosity vs. rotational speed is more important when entrance temperature is low.

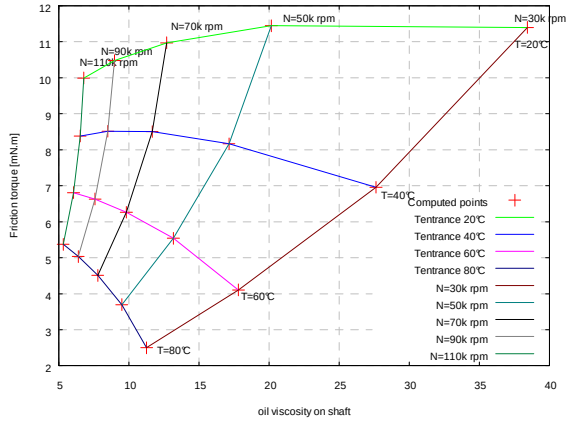

Figure 29 : Thermal friction torque vs. oil viscosity on shaft with constant entrance temperature and rotational speed

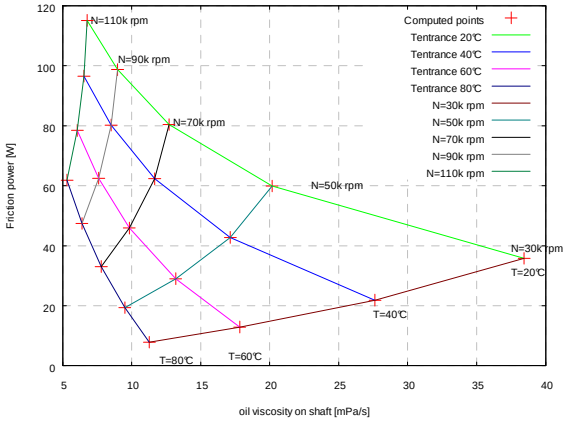

Figure 30 : Thermal friction power vs. oil viscosity on shaft with constant entrance temperature and rotational speed

4.CONCLUSION

This study proposes a model of friction losses in turbocharger bearings which seems close to the experimental results and may be useful in predicting friction losses due to the journal bearing. A new test rig/bench equipped with torquemeter is being developed and new experiments are planned to check the validity of the hypotheses and to further validate the results. This model will be enhanced with heat transfer through the shaft due to the environment of the turbocharger.

On the other hand, to predict global turbocharger performances, a model of the thrust bearing performances will be developed. This model will be validated by experiments on the CNAM test rig with a new and original solution for controlling axial charge on the thrust bearing.

REFERENCES

[1] Podevin, G. Descombes, V. Hara, A. Clenci, C. Zaharia. *Performances of turbochargers at low speeds,* EAEC, Belgrade, 2005.

[2] Osborne Reynolds. *On the Theory of Lubrication and Its Application to Mr. Beauchamp Tower's Experiments,* Philosophical Transactions of the Royal Society of London, Vol. 177 (1886), pp. 157-234

[3] S. Schmitt, W. Schmid, G. Hertweck, M.Schlegl, S. Staudacher. *Hochpräzise Messungen der Reibleistungen von Abgasturboladern,* Aufladetechnische Konferenz, 2007.

[4] J. Frène. *Paliers et butées hydrodynamiques,* Techniques de l'Ingénieur B5 320

[5] Y. Konan, M. Deligant, C. Périlhon, P. Podevin, A. Clenci. *Estimation by calculation of mechanical power losses on automotive turbochargers.* SMAT, Craiova, 2008.

[6] P. Podevin, G. Descombes, A. Clenci, Z. Cătălin. Researches regarding mechanical efficiency evaluation at turbochargers. CONAT, Brasov, 2004